Power Control of Grid Connected Doubly Fed Induction Generator with Sensor-less Speed and Position Estimation Algorithm

Sumanth Gali

A Dissertation Submitted to
Indian Institute of Technology Hyderabad
In Partial Fulfillment of the Requirements for
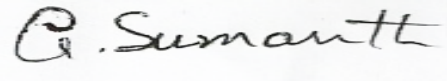The Degree of Master of Technology

भारतीय प्रौद्योगिकी संस्थान हैदराबाद
Indian Institute of Technology Hyderabad

Department of Electrical Engineering

June, 2014

Declaration

I declare that this written submission represents my ideas in my own words, and where others' ideas or words have been included, I have adequately cited and referenced the original sources. I also declare that I have adhered to all principles of academic honesty and integrity and have not misrepresented or fabricated or falsified any idea/data/fact/source in my submission. I understand that any violation of the above will be a cause for disciplinary action by the Institute and can also evoke penal action from the sources that have thus not been properly cited, or from whom proper permission has not been taken when needed.

(Signature)

Sumanth Gali

EE12M1016

Approval Sheet

This thesis entitled **Power Control of Grid Connected Doubly Fed Induction Generator with Sensor-less Speed and Position Estimation Algorithm** by **Sumanth Gali** is approved for the degree of Master of Technology from IIT Hyderabad.

R. Prasanth Kumar

-Name and affiliation-

Examiner

Ketan

-Name and affiliation-

IITH.

Examiner

K. Siva Kumar IITH

-Name and affiliation- SIVA KUMAR IITH

Adviser

Vaskar Sarkar, IITH

-Name and affiliation-

Co-Adviser

R. Prasanth Kumar

-Name and affiliation-

Chairman

Acknowledgements

Dedicated to

This work is dedicated to my beloved Lord's & my parents who have supported me throughout my education

Abstract

The aim of this thesis deals with the analysis, modeling and control of doubly-fed induction generator (DFIG) for wind turbines. The system uses two converters connected back to back, one is rotor side converter (RSC) or machine side converter and the other one is front end converter or grid side converter (GSC). The rotor side converter controls the active and reactive power by controlling the d-q components of rotor current (i.e.i_{rd} and i_{rq}). While the grid side converter controls the dc-link voltage and ensures the operation at unity power factor by making the reactive power drawn by the system from the utility grid to zero

In this thesis initially a control scheme which uses PI controller for power control of doubly-fed induction generator is discussed. The PI control scheme has high oscillations in the rotor injected voltages. To address this issue Feedback Linearization Control (FBLC) scheme is adopted. Analysis and simulations of both the methods is presented in this work.

In this work using sensor less algorithm speed and rotor position are estimated. The algorithm does not involve integration, recursive techniques, recompilations or programmable low-pass filters, etc. Starting on the fly, accurate computation near and through the synchronous speed, immunity against fluctuations in the grid voltage, and frequency are the other advantages of the algorithm. The algorithm should enable tracking of rotor position and speed accurately in a stable manner at any speed in the working range including the synchronous speed

List of figures

List of tables

Abbreviations

DFIG	Doubly Fed Induction Generator
GSC	Grid Side Converter
RSC	Rotor Side Converter
FBLC	Feedback Linearization Control

Nomenclature

Symbol	Definition	Units
α,β	Stationary reference frame	
d,q	Synchronously Rotating Reference Frame	
_a,_b	Rotor Reference Frame	
a,b,c	Three phase quantities	
v_S	Stator voltage vector………………	V
$|v_s|$	Stator voltage vector magnitude……	V
v_{ga} , v_{gb}, v_{gc}	Grid phase voltages…………………	V
v_{sa} , v_{sb}, v_{sc}	Stator phase voltages…………	V
$v_{g\alpha}$, $v_{g\beta}$	α and β axes grid voltages……..	V
$v_{s\alpha}$, $v_{s\beta}$	α and β axes Stator voltages……	V
v_{gd}, v_{gq}	d and q axes gird voltage…..	V
v_{sd}, v_{sq}	d and q axes Stator voltages…….	V
v_r	Rotor voltage vector….	V
v_{ra} , v_{rb}, v_{rc}	Rotor phase voltages…	V
$v_{r\alpha}$, $v_{r\beta}$	α and β axes Rotor voltages….	V
v_{rd}, v_{rq}	d and q axes Rotor voltages…	V
i_S	Stator current vector…..	A
i_{sa} , i_{sb}, i_{sc}	Stator phase currents….	A
$i_{s\alpha}$, $i_{s\beta}$	α and β axes Stator currents…	A
i_{sd}, i_{sq}	d and q axes stator currents….	A
i_r	Rotor current vector…..	A
i_{ra} , i_{rb}, i_{rc}	Rotor phase currents…..	A
$i_{r\alpha}$, $i_{r\beta}$	α and β axes Rotor currents…	A
i_{rd}, i_{rq}	d and q axes rotor currents….	A
i_{r_a}, i_{r_b}	a and b axes rotor currents…	A
v_{fe}	Front-end converter voltage vector	V
v_{fea} , v_{feb}, v_{fec}	Front-end converter phase voltages	V
v_{fed} , v_{feq}	d and q axes front-end converter voltage	V

i_{fe}	Front-end converter current vector	A
$i_{fea}, i_{feb}, i_{fec}$	Front-end converter phase currents	A
i_{fed}, i_{feq}	d and q axes front-end converter currents	A
v_{ac}	Stepped down grid voltage vector	V
v_{acd}, v_{acq}	d and q axes stepped down grid voltages	V
u_{fed}, u_{feq}	d and q axes voltages generated from front End converter loops	V
v_{fed}^*, v_{feq}^*	d and q axes reference voltages used for pulse Generation for front end converter	V
u_{rd}, u_{rq}	d and q axes voltages generated from rotor side Converter loops	V
v_{rd}^*, v_{rq}^*	d and q axes reference voltages used for pulse Generation for rotor side converter	V
v_{dc}	DC link voltage	V
i_{dc}	DC link current	A
i_L	DC link load current	A
i_C	DC link capacitor current	A
i_{rd}^*, i_{rq}^*	d and q axes rotor current reference	A
i_{fed}^*, i_{feq}^*	d and q axes front-end converter current Reference	A
v_{dc}^*	DC link voltage reference	V
R_s, R_r	Stator and rotor phase winding resistance	ohm
L_s, L_r	Stator and rotor phase winding inductance	H
L_m	Mutual magnetizing inductance	H
L_{ls}, L_{lr}	Stator and rotor self inductance	H
R_{fe}	Line side resistance	ohm
L_{fe}	Line side inductance	H
X_{fe}	Line side reactance	ohm
C	DC link capacitance	F
θ_s	Angle b/w stator voltage vector and β-axis	rad

θ_r	Actual rotor position	rad
θ_1	Angle b/w rotor current vector and β-axis	rad
θ_2	Angle b/w rotor current vector and _b-axis	rad
μ	Angle b/w stator flux magnetizing current Vector and β-axis	rad
ε	Estimated rotor position	rad
T_L	Load torque	N-m
T_e	Electromagnetic torque	N-m
ω_e	Angular velocity of stator voltage vector	rad/s
ω_r	Angular velocity of rotor	rad/s
$\omega_{r(est)}$	Estimated angular velocity of rotor	rad/s
J	Moment of inertia	Kg-m2
P	Number of poles	
t	Time	second
K_{11}, K_{12}	Gains are used in current control loop of Front end converter	
K_{21}, K_{22}, K_{23}	Gains are used in voltage control loop of Front end converter	
$E_1(x)$	Decoupling matrix used in front end converter	
$A_1(x)$	Control matrix used in front end converter	
K_{31}, K_{32}	Gains are used in d-axis current control loop of Rotor side converter	
K_{41}, K_{42}	Gains are used in q-axis current control loop of Side converter	
$E_2(x)$	Decoupling matrix used in rotor side converter	
$A_2(x)$	Control matrix used in rotor side converter	
P_s	Stator active power	W
P_s^*	Reference stator active power	W
Q_s	Stator reactive power	VAR
Q_s^*	Reference stator reactive power	VAR
P_r	Rotor active power	W

Q_r	Rotor reactive power	VAR
P_{in}	Active power flow into the system from grid	W
P_{out}	Active power flow out of the system to grid	W
s	Slip	

Contents

Chapter 1

INTRODUCTION

1.1 Introduction

Now a days due to efficient control of electric power, both at the generation and utilization ends. A major share of this power is generated and utilized through electromechanical energy conversion. This conversion of power in a controlled manner is achieved through variable speed operation of electrical machines. With the availability of power semiconductor devices the efficiency of conversion has become very high and also if desired, fast dynamic response can be achieved. In induction machines especially squirrel cage have become increasingly popular due to their rugged construction and maintenance-free operation

While squirrel cage rotor induction machines are mainly used for small and medium power drive applications, the wound rotor or slip-ring induction machines are commonly used in large power drives having limited range of operating speeds. Though the cost of a slip-ring machine is more than the squirrel cage machine, it is justified by the reduced size of power electronic converter in the rotor circuit. However, with the emergence of Variable Speed Constant Frequency (VSCF) generation applications such as wind power generation, there is an increased attention towards wound rotor induction machines.

1.2 Literary Review

1. The sensor less algorithm for finding out the speed and rotor position estimation are presented. The algorithm should enable tracking of rotor position and speed accurately in a stable manner at any speed in the working range including the synchronous speed. Secondly it should be able to start and function instantaneously when commanded or commissioned irrespective of the instant of commissioning

2. Here the Introduction of double-fed induction generator and its operation are explained in detail for applications like wind farms which need high power drives. The working principal, four quadrants operation, modeling of rotor side converts and grid side converter are presented

1

3. The method proposed here is to control the active and the reactive power by means of the rotor current control with angle controllers. This controllers produce directly the rotor currents with the desired frequency without rotor position measurement and coordinate transformations. The active and reactive power control is the presented simulation results.

4. A fast voltage PWM control strategy applying feedback linearization technique for three phase AC/DC grid side converter is proposed and implemented here. Incorporating the power balance of the input and output sides in system modeling, a nonlinear model of the PWM converter is derived with state variables such as ac input currents and dc output voltage.

5. A nonlinear control strategy based on its decoupled vector control model is proposed in this paper for DFIG. By using the feedback linearization, the control algorithm is established for rotor side converter only

6. Here complete machine modeling of doubly-fed induction generator and mathematical modeling of front end converter as well as rotor side converter are presented by using the voltage and current equations for the double-fed induction machine

1.3 Aim of thesis

The objective of the thesis is to develop a control scheme for the decoupled control of the active and reactive powers of the grid connected doubly-fed wound rotor induction machine including Speed and Rotor position estimation. In this context the mathematical model of the DFIG and the front end converter is developed. The control strategy for the front end and rotor side converters is developed. The effectiveness of the control scheme is observed by simulation using MATLAB/SIMULINK. Both control scheme using PI controller and FBLC are compared wherein with FBLC less oscillations in the reference rotor current are observed.

1.4 Outline of the thesis

The thesis is divided into seven chapters and each chapter deals with one of the major aspects.

Chapter 1

This chapter describes basics concepts of all the thesis work which is presented here

Chapter 2

This chapter describes in detail the overview of the operating principle, modes of operation and advantages of a doubly-fed wound rotor induction machine.

Chapter 3

In This chapter the mathematical modeling of the grid-connected DFIG system in synchronous reference frame and power control by PI Tuning is described in detail.

Chapter 4

This chapter presents the principle of FBLC and derivation of the control laws for the DFIG system using FBLC

Chapter 5

This chapter presents a simple and implicit sensor less algorithm for estimating the rotor position and speed of the double fed induction machine.

Chapter 6

This chapter discusses the simulation results of the DFIG system with PI, FBLC control technique including Speed and rotor position estimation

Chapter 7

The important conclusions out of this dissertation work are presented.

Chapter 2

Grid Connected Double-Fed Wound Rotor Induction Machine

2.1 Introduction

The most common machine which is widely used in these days is doubly fed induction generators (DFIG). It consists a Wound rotor Induction generator with open rotor terminals and Back to Back converters. The behavior of Doubly-Fed Induction Generator (DFIG) used with wind turbines to extract wind energy and transfer it to the grid. The DFIG has two connections to the grid- a direct connection to the main terminals of the stator windings, and a connection to the wound rotor windings via back-to-back voltage source converters. Reference [2]-[3] are explained about double fed induction generator.

2.2 Principle of operation

For a doubly-fed wound rotor induction machine, it is possible to accomplish independent control of active and reactive powers through current injection in the Rotor circuit in a desired manner. This can be carried out via the appropriate switching control of rotor side converters. With an IGBT converter in the rotor circuit, rotor terminals can be fed with three-phase currents of variable amplitude, frequency and phase. This enables reversible flow of active power in the rotor. the dc link capacitor being a source of reactive power, can assist stator side by sharing partially or fully the magnetizing current requirement of the machine.

Due to the bi-directional control capability of active and reactive powers, the operating range in the torque-speed plane spreads out on either side of synchronous speed implying both sub-synchronous and super-synchronous mode of operation. Moreover, the machine can operate in both motoring and generating modes. All the four quadrants of operation are

possible. This is described in Fig. 2.1. The rating of the converter depends on the desired speed range.

The main features of this configuration are listed below:

- Reduced converter cost, as they have to be rated for slip power only.
- System efficiency is improved, due to reduced losses in the converters.

2.3 Mode of operation:

The doubly-fed configuration of wound rotor induction machine has the capability to operate both in sub-synchronous and super-synchronous speeds and this is true for both motoring and generation.
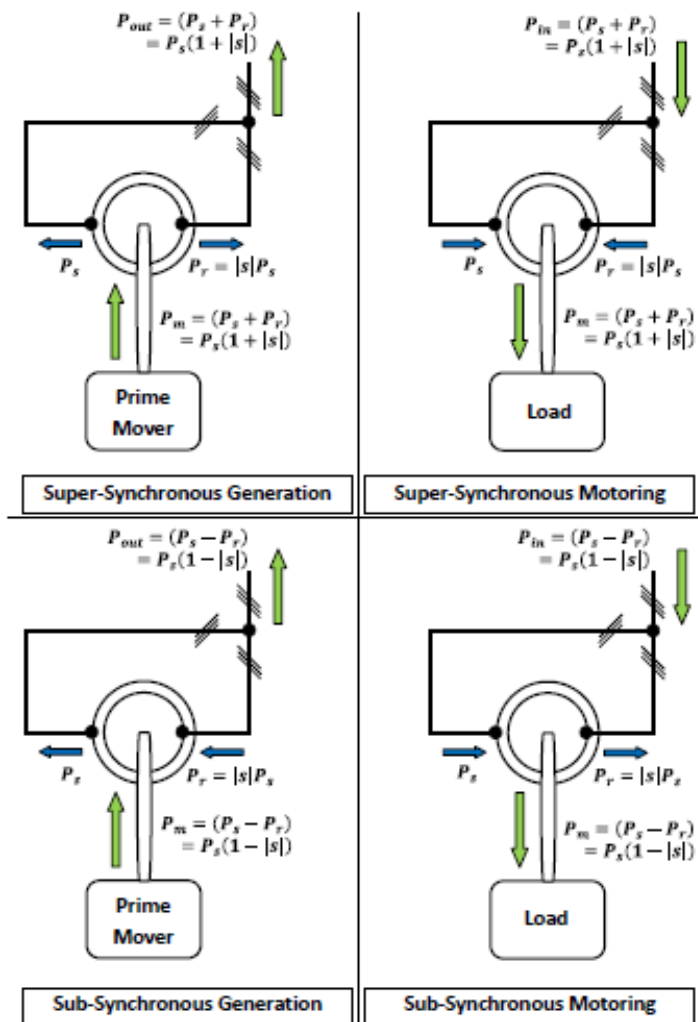

Fig 2.1 Power flow in all modes of operation

Mode1: In sub synchronous motoring mode, the stator draws power (P_s) from grid side and rotor power (P_r) which is equal to slip times of stator power is transferred to the converters to compensate the converter losses. Totally, the power ($P_s - P_r$) is supplied to the machine from grid. However we can control the rotor power (P_r) by using rotor side converter (RSC) to change the mode of operation if required.

Fig 2.2 Sub synchronous motoring mode

Mode2: In super synchronous generation mode, the stator power (P_s) is given to grid and rotor power (P_r) which is equal to slip times of stator power is transferred to the converters to compensate the converter losses. Totally, the power ($P_s + P_r$) is supplied to the grid. Here we can control the rotor power (P_r) by using rotor side converter (RSC) to change the mode of operation if required
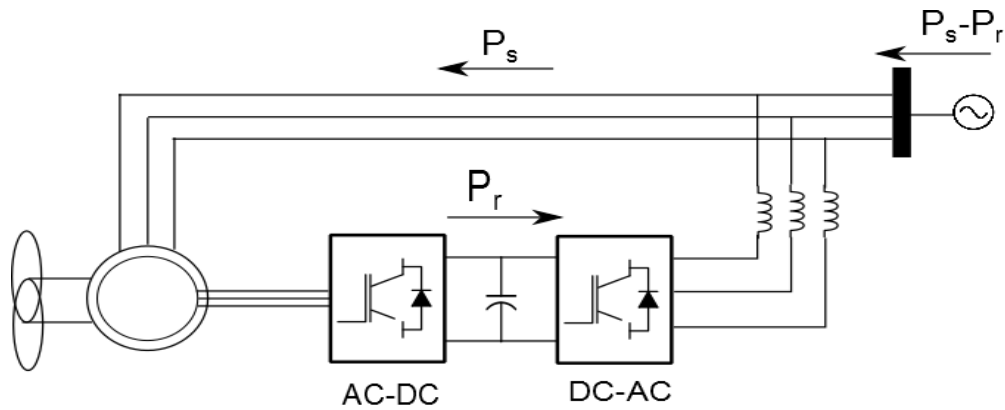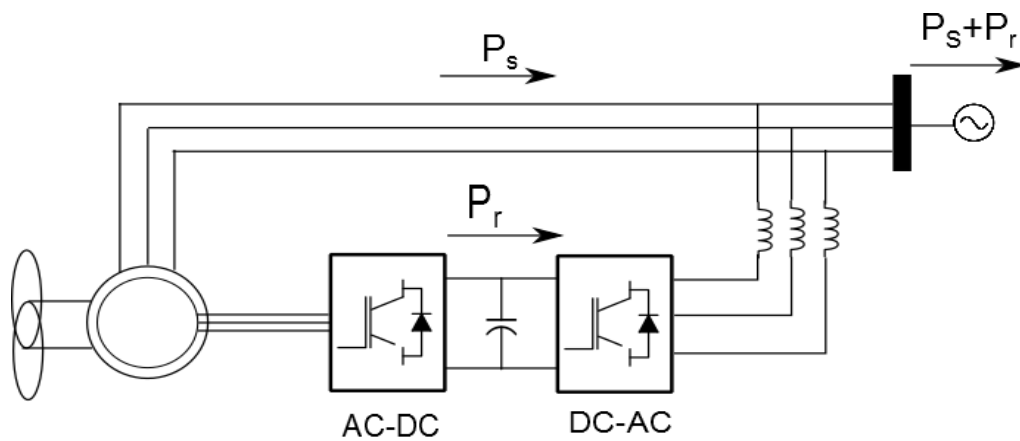

Fig 2.3 Super synchronous generation mode

Mode3: In sub synchronous generation the stator power (P_s) is transferring from grid side and rotor power (P_r) which is equal to slip times of stator power is coming to the converters to compensate the converter losses. Totally, the power ($P_s - P_r$) is supplied to the grid. Here we have to inject the rotor power (Pr) by using rotor side converter (RSC) to change the mode of operation if required

Fig 2.4 Sub synchronous generation mode

Mode4: In super synchronous motoring mode, the stator power (P_s) coming from grid side and rotor power (P_r) which is equal to slip times of stator power is coming to the converters to compensate the converter losses. Totally, the power ($P_s + P_r$) is supplied to the machine from grid. Here we have to inject the rotor power (P_r) by using rotor side converter (RSC) to change the mode of operation if required.
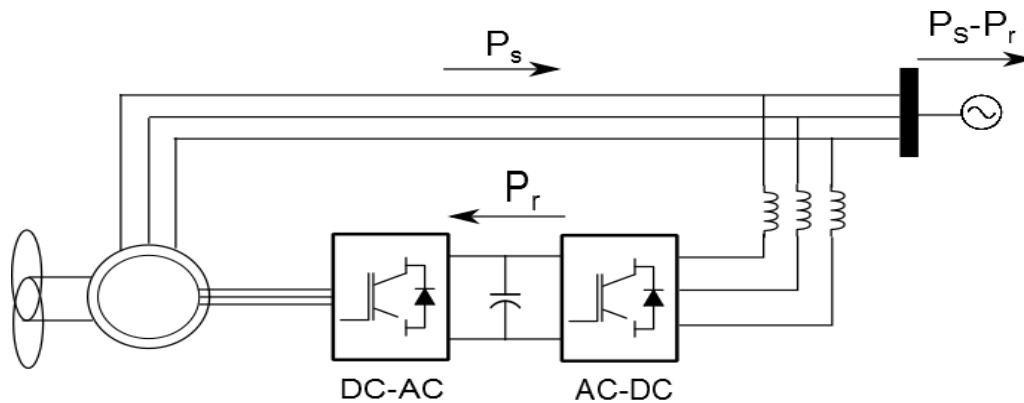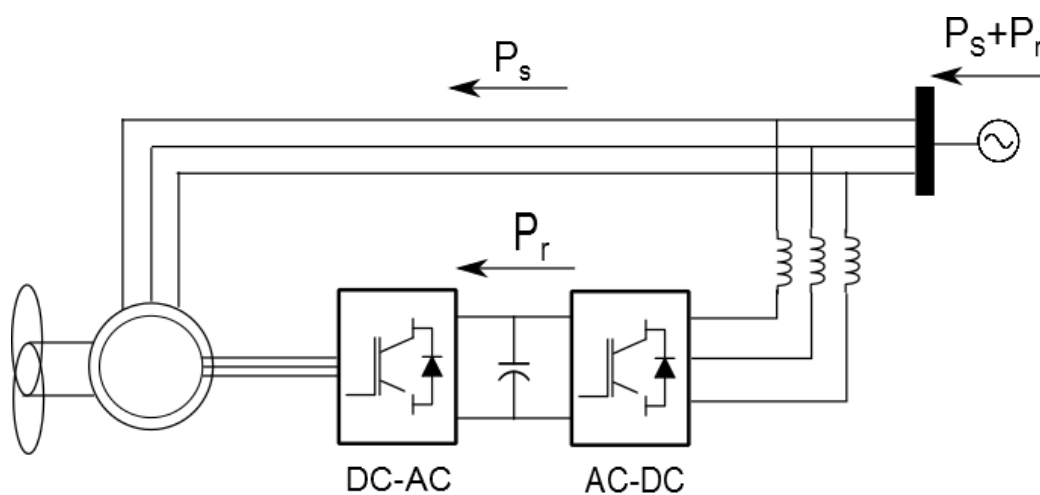

Fig 2.5 Super synchronous motoring mode

Chapter 3

Modeling & Power control (PI)

3.1 Introduction

In this chapter the complete modeling and simulation of wind turbine driven doubly-fed induction generator which feeds ac power to the utility grid. For that, two pulse width modulated voltage source converters are connected back to back between the rotor terminals and utility grid via common dc link. The grid side converter controls the power flow between the DC bus and the AC side and allows the system to be operated in sub-synchronous and super synchronous mode of operation. Reference [4]-[6]. The complete system is modeled and simulated in the MATLAB Simulink.

3.2 Mathematical modeling of wound rotor induction machine

The mathematical model of a general symmetrical ac machine (3.1 to 3.4) can be extended to obtain the model for doubly-fed induction machine.
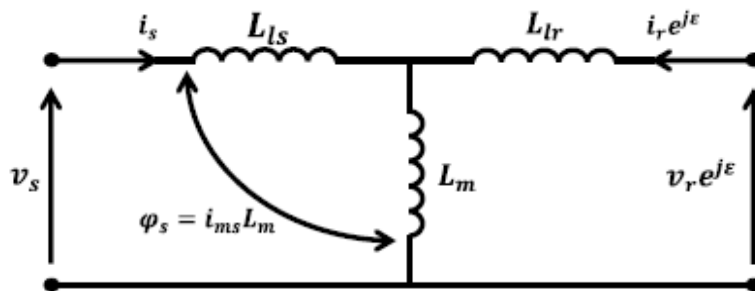

Fig. 3.1. Simplified single phase equivalent circuit of doubly-fed induction machine.

$$v_s(t) = R_s i_s + L_s \frac{d}{dt}(i_s) + L_m \frac{d}{dt}(i_r e^{j\varepsilon}) \qquad (3.1)$$

$$v_r(t) = R_r i_r + L_r \frac{d}{dt}(i_r) + L_m \frac{d}{dt}(i_s e^{j\varepsilon}) \qquad (3.2)$$

$$J\frac{d}{dt}(\omega_r) = T_e(t) - T_L(t) = \frac{3}{2}\frac{P}{2}L_m I_m\left[i_s\left(i_r e^{j\varepsilon}\right)^*\right] - T_L(t) \tag{3.3}$$

$$\frac{d}{dt}(\varepsilon) = \omega_r \tag{3.4}$$

Equations 3.1 and 3.2 describe the stator and rotor voltages (instantaneous) in the stator reference frame and rotor reference frame respectively. The electromagnetic torque is described by 3.3 and rotary motion is described by 3.4

3.2.1. Dynamic modeling of induction machine in the synchronous reference frame

The stator voltage equations for the machine in the stationary reference frame can be written as,

$$v_{s\alpha} = R_s i_{s\alpha} + \frac{d}{dt}\varphi_{s\alpha} \tag{3.5}$$

$$v_{s\beta} = R_s i_{s\beta} + \frac{d}{dt}\varphi_{s\beta} \tag{3.6}$$

Where $\varphi_{s\alpha}$ and $\varphi_{s\beta}$ are α-axis and β-axis stator flux linkages, respectively. When 3.5 and 3.6 are converted to synchronous reference frame, they can be written as,

$$v_{sq} = R_s i_{sq} + \frac{d}{dt}\varphi_{sq} + \omega_e\varphi_{sd} \tag{3.7}$$

$$v_{sd} = R_s i_{sd} + \frac{d}{dt}\varphi_{sd} - \omega_e\varphi_{sq} \tag{3.8}$$

If the rotor is not moving, that is if $\omega_r = 0$, the voltage equations for the rotor of a doubly fed wound rotor machine will be similar to the stator equations

$$v_{rq} = R_r i_{rq} + \frac{d}{dt}\varphi_{rq} + \omega_e\varphi_{rd} \tag{3.9}$$

$$v_{rq} = R_r i_{rd} + \frac{d}{dt}\varphi_{rd} - \omega_e\varphi_{rq} \tag{3.10}$$

Where all the variables and parameters are referred to the stator. Since the rotor actually moves at speed ω_r, the d-q axes move at a speed $(\omega_e - \omega_r)$ relative to the rotor. Therefore, in d-q frame, the rotor equations should be modified as,

$$v_{rq} = R_r i_{rq} + \frac{d}{dt}\varphi_{rq} + (\omega_e - \omega_r)\varphi_{rd} \tag{3.11}$$

$$v_{rd} = R_r i_{rd} + \frac{d}{dt}\varphi_{rd} - (\omega_e - \omega_r)\varphi_{rq} \tag{3.12}$$
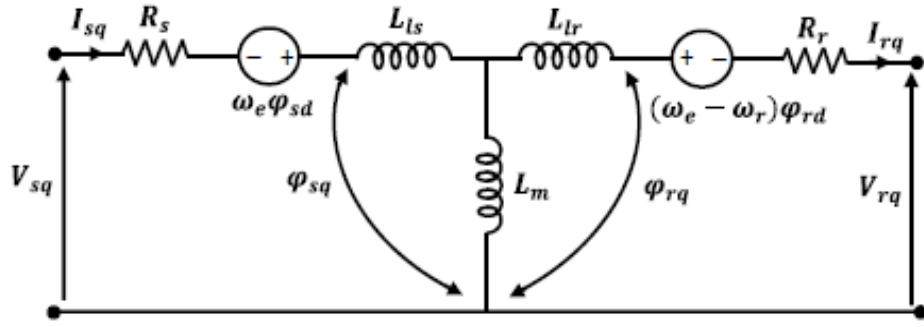
Fig. 3.2. q-axis equivalent of the induction machine in the synchronous reference frame.
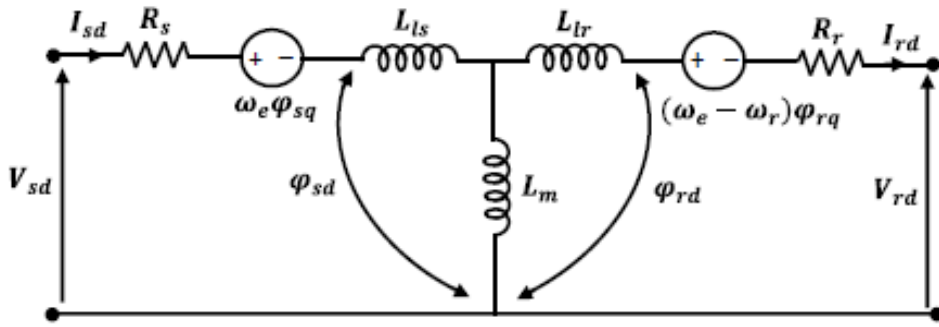

Fig. 3.3. d-axis equivalent of the induction machine in the synchronous reference frame.

Figs. 3.2 and 3.3 show the equivalent circuit of the induction machine in the synchronous reference frame. A special feature of the d-q model of the machine in the synchronous reference frame is that all the electrical variables appear as dc quantities in steady state.

The flux linkage expressions in terms of the currents can be written as,

$$\varphi_{sq} = L_{ls}i_{sq} + L_m(i_{sq} + i_{rq}) \tag{3.13}$$

$$\varphi_{rq} = L_{lr}i_{rq} + L_m(i_{sq} + i_{rq}) \tag{3.14}$$

$$\varphi_{mq} = L_m(i_{sq} + i_{rq}) \tag{3.15}$$

$$\varphi_{sd} = L_{ls}i_{sd} + L_m(i_{sd} + i_{rd}) \tag{3.16}$$

$$\varphi_{rd} = L_{lr}i_{rd} + L_m(i_{sd} + i_{rd}) \tag{3.17}$$

$$\varphi_{md} = L_m(i_{sd} + i_{rd}) \tag{3.18}$$

Conversely, the currents can be written in terms of the flux linkages as,

$$\begin{bmatrix} i_{sq} \\ i_{sd} \\ i_{rq} \\ i_{rd} \end{bmatrix} = \frac{1}{D} \begin{bmatrix} L_s & 0 & -L_m & 0 \\ 0 & L_s & 0 & -L_m \\ -L_m & 0 & L_r & 0 \\ 0 & -L_m & 0 & L_r \end{bmatrix} \begin{bmatrix} \varphi_{sq} \\ \varphi_{sd} \\ \varphi_{rq} \\ \varphi_{rd} \end{bmatrix} \tag{3.19}$$

Where $D = L_s L_r + L_m^2$

The relationship between the speed ω_r and the torque is given by,

$$T_e = T_L + J\frac{d\omega_m}{dt} + B\omega_m = T_L + \frac{2}{P}J\frac{d\omega_r}{dt} + \frac{2}{P}B\omega_r \tag{3.20}$$

Where T_L is load torque, J is the combined moment of inertia of rotor and load, B is coefficient of friction, P is number of poles, ω_m is rotor angular velocity (mechanical rad/s) and ω_r is rotor angular velocity (electrical rad/s).

The developed electromagnetic torque T_e in d-q variables is given as,

$$T_e = \frac{3}{2}\left(\frac{P}{2}\right) L_m (i_{sq} i_{rd} - i_{sd} i_{rq}) \tag{3.21}$$

3.3. Mathematical modeling of the rotor side converter

The rotor side converter is connected to the windings on the rotor of the induction machine. It injects the voltages into the rotor at the slip frequency. So the equations for rotor side converter are

$$v_{rd} = R_r i_{rd} + \frac{d}{dt}(L_r i_{rd} + L_m i_{sd}) - (\omega_e - \omega_r)(L_r i_{rq} + L_m i_{sq}) \tag{3.22}$$

$$v_{rq} = R_r i_{rq} + \frac{d}{dt}(L_r i_{rq} + L_m i_{sq}) - (\omega_e - \omega_r)(L_r i_{rd} + L_m i_{sd}) \tag{3.23}$$

3.4. Mathematical modeling of front end converter

The front side converter is connected to the directly to the Grid. So the voltage equations for front end converter are

$$\left(\frac{L_{fe}}{R_{fe}}\right)\frac{d}{dt}\left(i_{feq}\right) + i_{feq} = -\frac{v_{feq}}{R_{fe}} + \frac{v_{acq}}{R_{fe}} - \left(\frac{L_{fe}}{R_{fe}}\right)\omega_e i_{fed} \tag{3.24}$$

$$\left(\frac{L_{fe}}{R_{fe}}\right)\frac{d}{dt}\left(i_{fed}\right) + i_{fed} = -\frac{v_{fed}}{R_{fe}} + \left(\frac{L_{fe}}{R_{fe}}\right)\omega_e i_{feq} \tag{3.25}$$

3.5 Power control

In DFIG two types of converters one is Rotor Side Converter (RSC) another is Front-end Converter or Grid Side Converter (GSC) which are connected "back-to-back." Between the two converters a dc-link capacitor is placed. In Grid side converter control the voltages and currents reference is comparing to the actual values after that tuning PI controller. We get the Voltage references of grid side converter. Similarly in Rotor side converter (RSC) also the currents reference is comparing to the actual values after tuning we get rotor side converter control voltage references.

3.5.1 Control of Grid Side Converter

The Grid Side Converter is a voltage source inverter which serves as an interface to connect the dc-link of the doubly-fed machine. The control of the Grid Side Converter enables bidirectional flow of power and maintains dc-link voltage constant. The dc-link capacitor acts as source of reactive power. Also as the converter works in current controlled mode

Objectives of front end converter:

> To regulate the dc-link voltage
> Bidirectional power flow
> Fast dynamics response

The voltage equations of grid side converter are

$$u_{fed} = R_{fe}i_{fed} - \omega_e L_{fe}i_{feq} + L_{fe}v_{f1}$$

$$u_{feq}$$
$$= R_{fe}i_{feq} - \omega_e L_{fe}i_{fed} + \frac{2CL_{fe}v_{dc}}{3E}v_{f2} + \frac{2L_{fe}v_{dc}}{3E}i_L + \frac{L_{fe}}{v_{dc}}i_{feq}\left\{\frac{3}{2Cv_{dc}}Ei_{feq} - \frac{i_L}{C}\right\}$$

Since

$$u_{fed} = v_{acd} - v_{fed} \qquad u_{feq} = v_{acq} - v_{feq}$$

The resultant voltage reference to be modulated by the Grid Side Converter are given

$$v_{fed}^* = v_{acd} - u_{fed} = -u_{fed}$$

$$v_{feq}^* = v_{acq} - u_{feq}$$

3.5.2 Control of Rotor Side Converter

The main purpose of the machine side converter or Rotor Side Converter is to maintain the rotor speed constant irrespective of the wind speed and also the control strategy had been implemented to control the active power and reactive power flow of the machine using rotor currents components.

➢ The active power flow is controlled through i_{rd}
➢ The reactive power flow is controlled through i_{rq}
➢ To ensure unit power factor operation like grid side converter the reactive power demand is set to zero

The voltage equations of rotor side converter are

$$u_{rd} = R_r i_{rd} - \omega_2 \sigma L_r i_{rq} + \sigma L_r v_1$$

$$u_{rq} = R_r i_{rq} + \omega_2 \sigma L_r i_{rd} + \frac{\omega_2 L_0^2 i_{ms}}{L_s} + \sigma L_r v_2$$

The voltage u_{rd} and u_{rq} are the injecting voltages and these values are compared With actual values v_{rd} and v_{rq} respectively

$$v_{rd}^* = v_{rd} - u_{rd}$$

$$v_{rq}^* = v_{rq} - u_{rq}$$

Chapter 4

FBLC Controller for Grid Connected DFIG

4.1. Introduction

In doubly-fed motors, the stator is connected to a constant voltage and constant frequency source and the rotor is fed from a power converter. The stator flux oriented frame of reference is generally used for decoupling the active and reactive currents loops in case of doubly-fed machine.

PI controller based techniques have been reported in the literature. Although this technique is very simple, reliable and yields good performance, it is not very much effective for all operating conditions because, in general, one chosen set of PI-gains may not be best suited for all operating points. Moreover, the selection of gains for various PI controllers in power control of DFIG is tedious because of the inherent coupling between the d-axis and q-axis voltages. Also PI based control is based on a trial and error approach which is an imprecise task.

Feedback Linearization is a powerful technique that takes nonlinearities into account directly thus in the context of complex closed loop power control of DFIG which is a MIMO system, it is proposed to apply the feedback linearization control technique to achieve dynamic interaction between them. References [5]-[7]. An attempt has been made here to design a feedback linearization control technique for the power control of DFIG for enhanced power flow control.

This chapter focuses on a nonlinear multivariable control technique for controlling the operation of DFIG using feedback linearization approach. The feedback linearization technique is based on the idea of cancelling the non- linearity of the system and imposing the desired linear dynamics to control the system. Firstly, the principle of feedback linearization

control in general is explained and then using this principle, a non-linear control design is developed for the rotor side converter and front end converter.

4.2. Principle of Feedback Linearization Control (FBLC)

A non-linear control design using feedback linearization is presented here. Consider a multi-input multi-output (MIMO) system as follows

$$\dot{x} = f(x) + g(x)u \tag{4.1}$$

$$y = h(x) \tag{4.2}$$

Where

x is the State vector;

u is the array of control inputs;

y is the array of outputs;

f,g are smooth vector fields

h is a smooth scalar function

An approach to obtain the input-output linearization of the MIMO system is to differentiate the output 'y' of the system until the inputs appear. By differentiating second equation

$$\dot{y}_i = L_f h_i + \sum_{j=1}^{m} (L_{gj} h_i) u_j \tag{4.3}$$

Where $L_f h_i$ and $L_{gj} h_i$ represents Lie derivatives of h(x) w.r.t f(x) and g(x), respectively. If $L_{gj} h_i(x) = 0$ for all j, then the inputs do not appear and we have to differentiate respectively as

$$y_i^{(r_i)} = L_f^{(r_i)} h_i + \sum_{j=1}^{m} (L_{gj} L_f^{(r_i-1)} h_i) u_j \tag{4.4}$$

With $L_{gj} L_f^{r_i-1} h_i(x) = /0$ for at least one 'j'. If we perform the above procedure for each output 'y_i', we can obtain a total of 'm' equations in the above form, which can be written as

$$
\begin{bmatrix} y_1^{(r_1)} \\ \dots \\ \dots \\ y_m^{(r_m)} \end{bmatrix} = \begin{bmatrix} L_f^{(r_1)} h_1(x) \\ \dots \\ \dots \\ L_f^{(r_m)} h_m(x) \end{bmatrix} + E(x) \begin{bmatrix} u_1 \\ \dots \\ \dots \\ u_m \end{bmatrix} \tag{4.5}
$$

Where the m x m matrix E(x) is defined as

$$
E(x) = \begin{bmatrix} L_{g1}L_f{}^{(r_1-1)}h_1 & \cdots & \cdots & L_{gm}L_f{}^{(r_1-1)}h_1 \\ \vdots & \vdots & \vdots & \vdots \\ L_{g1}\,L_f{}^{(r_m-1)}h_m & \cdots & \cdots & L_{gm}L_f{}^{(r_m-1)}h_m \end{bmatrix}
\tag{4.6}
$$

The matrix E(x) is called the decoupling matrix for the MIMO system.

$$
u = -E^{-1}(x)\begin{bmatrix} L_f{}^{(r_1)}h_1(x) \\ \cdots \\ \cdots \\ L_f{}^{(r_m)}h_m(x) \end{bmatrix} + E^{-1}(x)\begin{bmatrix} v_1 \\ \cdots \\ \cdots \\ v_m \end{bmatrix}
\tag{4.7}
$$

Where [V1 … … Vm]T are the new sets of inputs defined by the designer. The resultant dynamics of the system with new control can be obtained

$$
\begin{bmatrix} y_1{}^{(r_1)} \\ \cdots \\ \cdots \\ y_m{}^{(r_m)} \end{bmatrix} = \begin{bmatrix} v_1 \\ \cdots \\ \cdots \\ v_m \end{bmatrix}
\tag{4.8}
$$

4.2.1. Feedback linearization Control of front end converter

With the dynamic behavior of the front end converter is expressed in the form eq-1 & eq-2, we obtain

$$
f(x) = \begin{bmatrix} f_1(x) \\ f_2(x) \\ f_3(x) \end{bmatrix} = \begin{bmatrix} -\dfrac{R_{fe}}{L_{fe}}x_1 + \omega_e x_2 \\ -\dfrac{R_{fe}}{L_{fe}}x_2 - \omega_e x_1 \\ \dfrac{3}{2Cx_3}Ex_2 - \dfrac{i_L}{C} \end{bmatrix}
\tag{4.9}
$$

$$g(x) = \begin{bmatrix} g_1(x) & 0 \\ 0 & g_2(x) \\ 0 & 0 \end{bmatrix} = \begin{bmatrix} \dfrac{1}{L_{fe}} & 0 \\ 0 & \dfrac{1}{L_{fe}} \\ 0 & 0 \end{bmatrix} \qquad (4.10)$$

$$x = \begin{bmatrix} x_1 \\ x_2 \\ x_3 \end{bmatrix} = \begin{bmatrix} i_{fed} \\ i_{feq} \\ v_{dc} \end{bmatrix} \qquad (4.11)$$

$$u = \begin{bmatrix} u_{fed} \\ u_{feq} \end{bmatrix} = \begin{bmatrix} v_{acd} - v_{fed} \\ v_{acq} - v_{feq} \end{bmatrix} \qquad (4.12)$$

Where E=Vacq and Vacd=0

Since there are two control inputs for the given system, we should have two outputs for input-output decoupling. One control input is used to regulate the input line current and the other is for the capacitor voltage. If the system is required to operate at unity power factor, the reactive component i_{fed} of the line current should be zero. Then, we choose the two outputs as

$$y_1 = x_1 = i_{fed} \qquad (4.13)$$

$$y_2 = x_3 = v_{dc} \qquad (4.14)$$

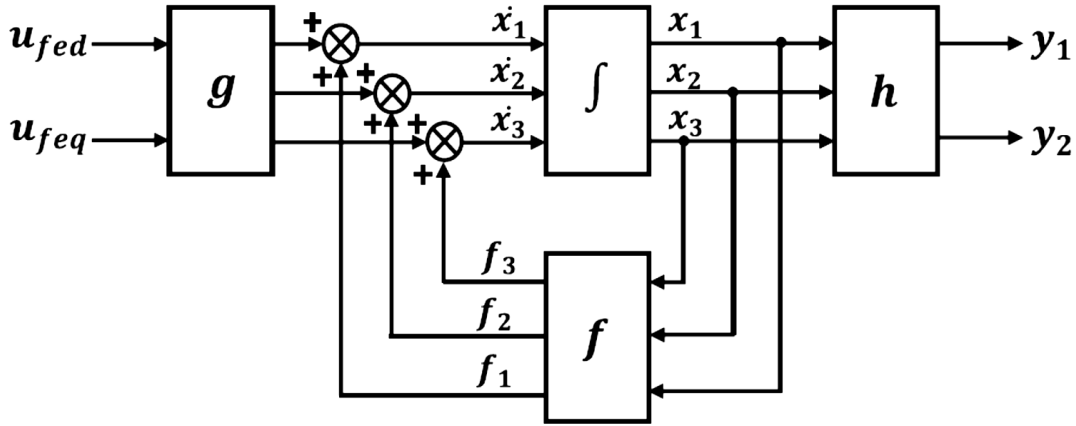the nonlinear model block diagram of the front end converter is

Fig.4.1   FBLC block diagram for front end converter

Differentiating y1 and y2 until a control input appears and arranging them in the form of (4.5)

$$\begin{bmatrix} \dot{y}_1 \\ \ddot{y}_2 \end{bmatrix} = A_1(x) + E_1(x) \begin{bmatrix} u_{fed} \\ u_{feq} \end{bmatrix} \qquad (4.15)$$

Where

$$A_1(x) = \begin{bmatrix} f_1 \\ \dfrac{3}{2Cv_{dc}}Ef_2 - \dfrac{3f_3}{2Cx_3^2}Ex_2 + \dfrac{i_L}{C} \end{bmatrix} \quad (4.16)$$

$$E_1(x) = \begin{bmatrix} g_1 & 0 \\ 0 & \dfrac{3Eg_2}{2Cx_3} \end{bmatrix} \quad (4.17)$$

From equation (4.22)

$$\begin{bmatrix} u_{fed} \\ u_{feq} \end{bmatrix} = E_1^{-1}(x)\left[-A_1(x) + \begin{bmatrix} v_{f1} \\ v_{f2} \end{bmatrix} \right] \quad (4.18)$$

Where

$$E_1^{-1}(x) = \begin{bmatrix} \dfrac{1}{g_1} & 0 \\ 0 & \dfrac{2Cx_3}{3Eg_2} \end{bmatrix} \quad (4.19)$$

For tracking control, the new control inputs are given by

$$\begin{bmatrix} v_{f1} \\ v_{f2} \end{bmatrix} = \begin{bmatrix} \dot{y}_{1ref} - k_{11}e_1 - k_{12}\int e_1\, dt \\ \ddot{y}_{2ref} - k_{21}\dot{e}_2 - k_{22}e_2 - k_{23}\int e_2\, dt \end{bmatrix} \quad (4.20)$$

Where $e_1 = y_1 - y_{1ref}$ and $\dot{e}_1 = \dot{y}_1 - \dot{y}_{1ref}$. Then, the output errors are governed by

$$\dot{e}_1 + k_{11}e_1 = 0 \quad (4.21)$$

$$\ddot{e}_2 + k_{21}\dot{e}_2 + k_{22}e_2 = 0 \quad (4.22)$$

Even through the nonlinear system can be linearized by exact feedback linearization, these may exist a tracking error in the presence of parameter variations. To eliminate this tracking error, we add integral controls to (4.20)

$$\begin{bmatrix} v_{f1} \\ v_{f2} \end{bmatrix} = \begin{bmatrix} \dot{y}_{1ref} - k_{11}e_1 - k_{12}\int e_1\, dt \\ \ddot{y}_{2ref} - k_{21}\dot{e}_2 - k_{22}e_2 - k_{23}\int e_2\, dt \end{bmatrix} \quad (4.23)$$

From (4.30), then we obtain error dynamics as

$$\ddot{e}_1 + k_{11}\dot{e}_1 + k_{12}e_1 = 0 \tag{4.24}$$

$$\dddot{e}_2 + k_{21}\ddot{e}_2 + k_{22}\dot{e}_2 + k_{23}e_2 = 0 \tag{4.25}$$

Substituting (4.23) into (4.18)

$$u_{fed} = R_{fe}i_{fed} - \omega_e L_{fe}i_{feq} + L_{fe}v_{f1} \tag{4.26}$$

$$u_{feq} = R_{fe}i_{feq} + \omega_e L_{fe}i_{fed} + \frac{2CL_{fe}v_{dc}}{3E}v_{f2} + \frac{2L_{fe}v_{dc}}{3E}i_L \tag{4.27}$$

$$+ \frac{L_{fe}}{v_{dc}}i_{feq}\left\{\frac{3}{2Cv_{dc}}Ei_{feq} - \frac{i_L}{C}\right\}$$

Since $u_{fed} = v_{acd} - v_{fed}$ and $u_{feq} = v_{acq} - v_{feq}$, the resultant voltage reference to be modulated by the front end converter are given

$$v_{fed}^* = v_{acd} - u_{fed} = -u_{fed} \tag{4.28}$$

$$v_{feq}^* = v_{acq} - u_{feq} \tag{4.29}$$

The current and voltage loops for the front end converter are shown in figure
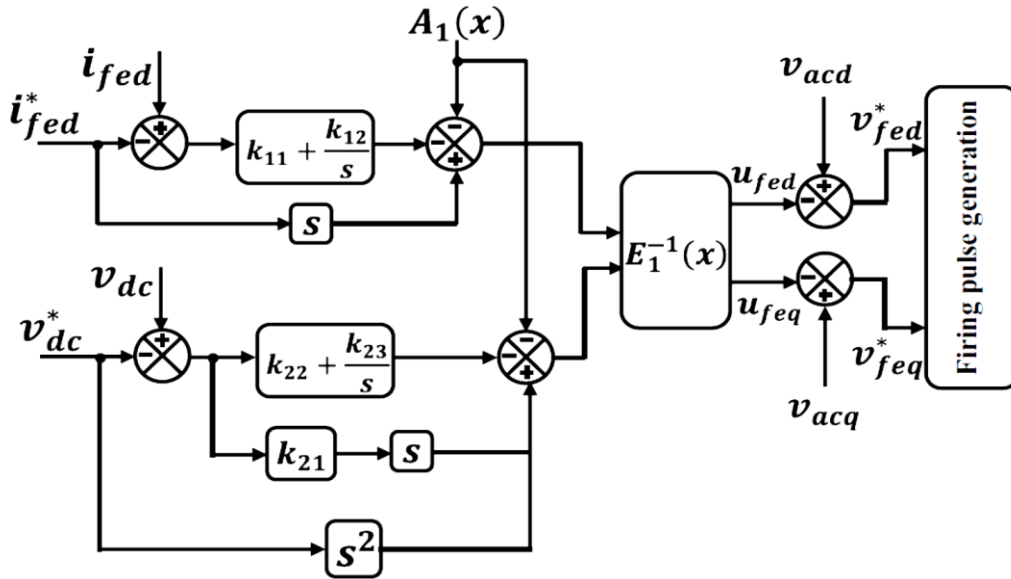
Fig.4.2 Current and voltage loops for front end converter

4.2.2. Feedback linearization Control of rotor side converter:

With the dynamic behavior of the rotor side converter is expressed in the form of (4.1) and (4.2) we obtain

$$f(x) = \begin{bmatrix} f_1(x) \\ f_2(x) \end{bmatrix} = \begin{bmatrix} -\dfrac{R_r}{\sigma L_r} x_1 + \omega_2 x_2 \\ -\dfrac{R_r}{\sigma L_r} x_2 - \omega_2 x_1 - \dfrac{\omega_2 L_0^2 i_{ms}}{L_s \sigma L_r} \end{bmatrix} \tag{4.30}$$

$$g(x) = \begin{bmatrix} g_1(x) & 0 \\ 0 & g_2(x) \\ 0 & 0 \end{bmatrix} = \begin{bmatrix} \dfrac{1}{\sigma L_r} & 0 \\ 0 & \dfrac{1}{\sigma L_r} \\ 0 & 0 \end{bmatrix} \tag{4.31}$$

$$x = \begin{bmatrix} x_1 \\ x_2 \end{bmatrix} = \begin{bmatrix} i_{rd} \\ i_{rq} \end{bmatrix} \tag{4.32}$$

$$u = \begin{bmatrix} u_{rd} \\ u_{rq} \end{bmatrix} \tag{4.33}$$

Since there are two control inputs for the given system, we should have two outputs for input-output decoupling. One control input is used to regulate the rotor d-axis current and the other is for the rotor q-axis current.

$$y_1 = h_1(x) = x_1 = i_{rd} \tag{4.34}$$

$$y_1 = h_2(x) = x_2 = i_{rq} \tag{4.35}$$

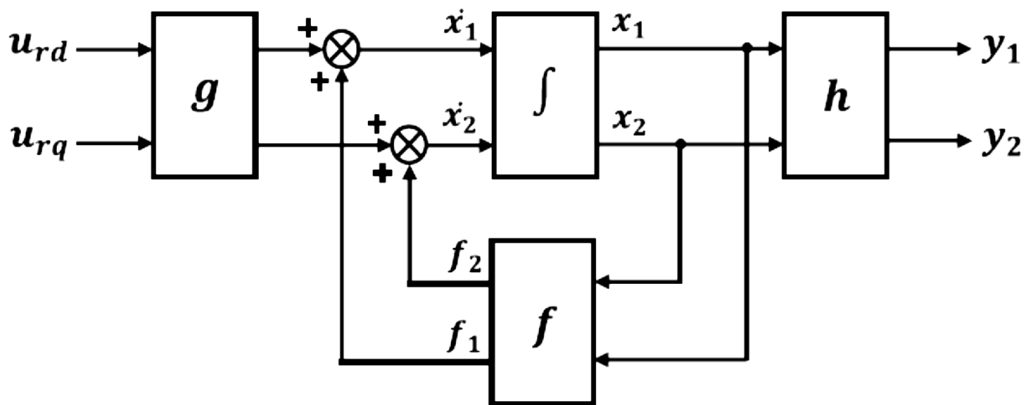The nonlinear model block diagram of the rotor side converter

Fig 4.3 FBLC block diagram for rotor side converter

Differentiating y1 and y2 until a control input appears and arranging them in the form
Of (4.5)

$$\begin{bmatrix} \dot{y}_1 \\ \ddot{y}_2 \end{bmatrix} = A_2(x) + E_2(x) \begin{bmatrix} u_{rd} \\ u_{rq} \end{bmatrix} \tag{4.36}$$

Where

$$A_2(x) = \begin{bmatrix} f_1 \\ f_2 \end{bmatrix} = \begin{bmatrix} -\dfrac{R_r}{\sigma L_r} x_1 + \omega_2 x_2 \\[4mm] -\dfrac{R_r}{\sigma L_r} x_2 - \omega_2 x_1 - \dfrac{\omega_2 L_0^2 i_{ms}}{L_s \sigma L_r} \end{bmatrix} \tag{4.37}$$

$$E_2(x) = \begin{bmatrix} g_1 & 0 \\ 0 & g_2 \end{bmatrix} = \begin{bmatrix} \dfrac{1}{\sigma L_r} & 0 \\[3mm] 0 & \dfrac{1}{\sigma L_r} \end{bmatrix} \tag{4.38}$$

From (4.36)

$$\begin{bmatrix} u_{rd} \\ u_{rq} \end{bmatrix} = E_2^{-1}(x) \left[-A_2(x) + \begin{bmatrix} v_{r1} \\ v_{r2} \end{bmatrix} \right] \tag{4.39}$$

Where

$$E_2^{-1}(x) = \begin{bmatrix} \dfrac{1}{g_1} & 0 \\[3mm] 0 & \dfrac{1}{g_2} \end{bmatrix} = \begin{bmatrix} \sigma L_r & 0 \\ 0 & \sigma L_r \end{bmatrix} \tag{4.40}$$

For tracking control, the new control inputs are given by

$$\begin{bmatrix} v_1 \\ v_2 \end{bmatrix} = \begin{bmatrix} \dot{y}_{1ref} - k_{31} e_1 \\ \dot{y}_{2ref} - k_{41} e_2 \end{bmatrix} \tag{4.41}$$

Where $e_1 = y_1 - y_{1ref}$ and $\dot{e}_1 = \dot{y}_1 - \dot{y}_{1ref}$. Then, the output errors are governed by

$$\dot{e}_1 + k_{31}e_1 = 0 \tag{4.42}$$

$$\dot{e}_2 + k_{41}e_2 = 0 \tag{4.43}$$

Even through the nonlinear system can be linearized by exact feedback linearization, these may exist a tracking error in the presence of parameter variations. To eliminate this tracking error, we add integral controls to (4.41)

$$\begin{bmatrix} v_1 \\ v_2 \end{bmatrix} = \begin{bmatrix} \dot{y}_{1ref} - k_{31}e_1 - k_{32}\displaystyle\int e_1 \; dt \\ \dot{y}_{2ref} - k_{41}e_2 - k_{42}\displaystyle\int e_2 \; dt \end{bmatrix} \tag{4.44}$$

From (4.44), then we obtain error dynamics as

$$\ddot{e}_1 + k_{31}\dot{e}_1 + k_{32}e_1 = 0 \tag{4.45}$$

$$\ddot{e}_2 + k_{41}\dot{e}_2 + k_{42}e_2 = 0 \tag{4.46}$$

Substituting (4.44) to (4.39)

$$u_{rd} = R_r i_{rd} - \omega_2 \sigma L_r i_{rq} + \sigma L_r v_1 \tag{4.47}$$

$$u_{rq} = R_r i_{rq} + \omega_2 \sigma L_r i_{rd} + \frac{\omega_2 L_0^2 i_{ms}}{L_s} + \sigma L_r v_2 \tag{4.48}$$

The voltages u_{rd} and u_{rq} are the injecting voltages and these values are compared with actual values v_{rd} and v_{rd} respectively.

$$v_{rd}^* = v_{rd} - u_{rd} \tag{4.49}$$

$$v_{rq}^* = v_{rq} - u_{rq} \tag{4.50}$$

The current loops for the rotor side converter are shown in figure
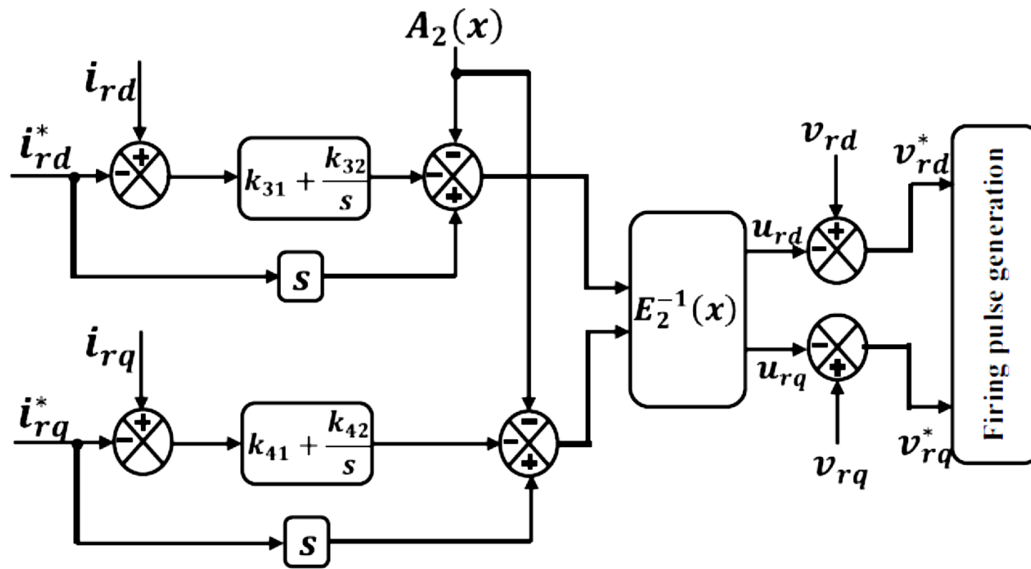
Fig 4.4 Current loops for rotor side converter

Chapter 5

Sensor less algorithm

5.1 Introduction

Doubly fed induction machine (DFIM) is a cost-effective alternative for variable-speed drives since a high dynamic performance can be archived with rotor side vector control and only a fraction of the machine nominal power needs to be processed by the power electronics converters. In such high-precision drives, sensor-less control is preferred because of the reduced cabling and hardware complexity, increased reliability, lower cost and low maintenance requirements. In [1]-[8] There are two major requirements in designing a position and speed sensor-less scheme for a vector-controlled wound rotor induction motor drive. Firstly, the algorithm should enable tracking of rotor position and speed accurately in a stable manner at any speed in the working range including the synchronous speed. Secondly it should be able to start and function instantaneously when commanded or commissioned irrespective of the instant of commissioning.

5.2 Spatial distributions of different space vectors:

The stator current i_s, the rotor current i_r and the stator voltage v_s, are used for the estimation of rotor position and speed. The spatial distribution of the stator voltage, stator magnetic flux and the rotor current vectors in different frames of reference are shown below. The total stator voltage vector is chosen to be aligned with the q-axis in the synchronous reference frame (i.e. $v_q=v_s$ and $v_d=0$), assuming the stator resistance drop to be negligible. Reference frame (i.e. $v_q=v_s$ and $v_d=0$), assuming the stator resistance drop to be negligible.

The rotor current i_r space vector makes an angle θ_1 w.r.t β-axis of stator reference frame and an angle θ_2 w.r.t _b-axis of rotor reference frame. Hence, the difference of angle θ_1 and θ_2 gives the required rotor position ε. The estimation algorithm is explaining in steps
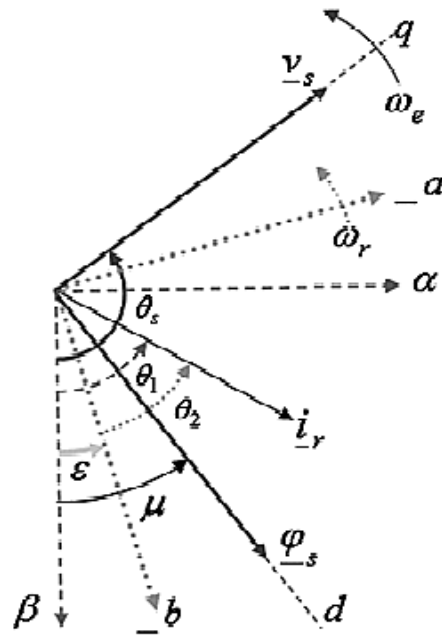

Fig 5.1 Spatial distributions of different space vectors

q-d------- Synchronous reference frame

_a,_b--- Rotor reference frame

$\alpha\beta$ ---- Stator reference frame

5.3 Implicit position-sensor less estimation:

➢ The stator current, the rotor current and the stator voltage, are used for the estimation of rotor position and speed.

➢ The Implicit position-sensor less estimation initially we get the rotor position and next the speed

➢ The difference of θ_1-θ_2 is the Position of rotor (ε).
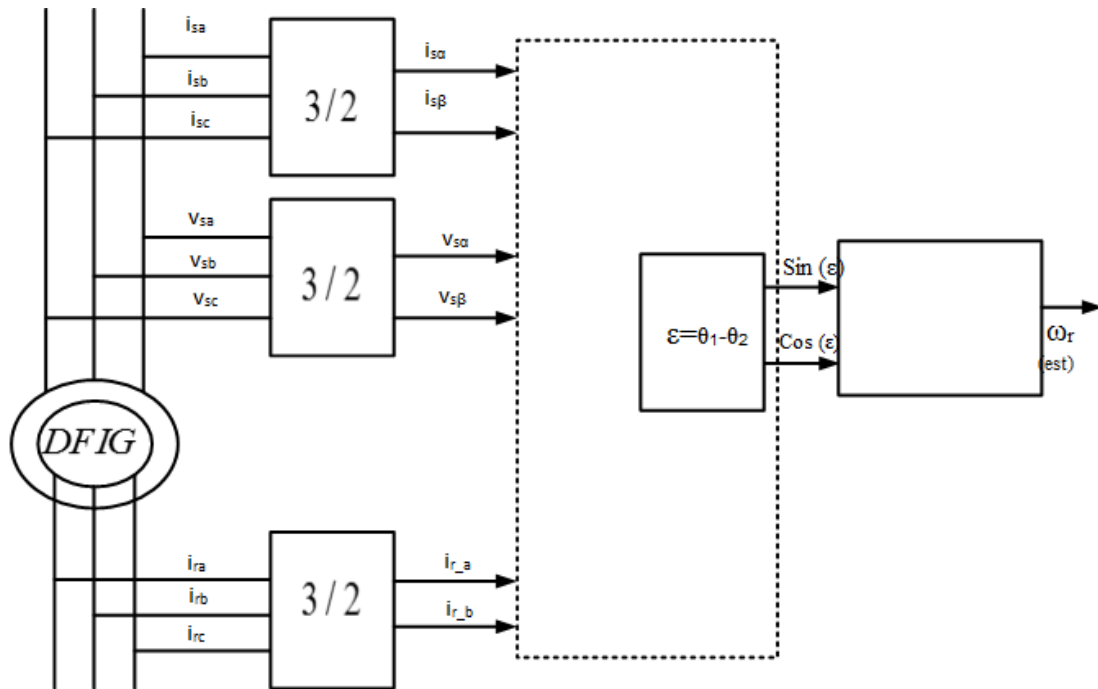
Fig 5.2 Implicit position-sensor less estimation

5.4 **Sensor less position estimation algorithm:**

<u>Step</u> 1: Here i_r in rotor reference frame (i_{r_a} and i_{r_b}) components of rotor current i_r in rotor reference frame can be computed using the a,b,c to _a,_b transformation. From these sin (θ_2) and cos (θ_2) can be computed

$$\text{Sin} (\theta_2) = \frac{i_{r\_a}}{\sqrt{(i_{r\_a}^2 + i_{r\_b}^2)}}$$

$$\text{Cos} (\theta_2) = \frac{i_{r\_b}}{\sqrt{(i_{r\_a}^2 + i_{r\_b}^2)}}$$

<u>Step</u> 2: i_r in rotor reference frame ($i_{r\alpha}$ and $i_{r\beta}$) the rotor current co-ordinates in the stationary reference frame can be computed in an implicit manner without the need of stator flux estimation. The rotor currents with respect to stationary reference frame are

$$i_{r\alpha} = \frac{R_s\, i_{s\beta} - v_{s\beta} - \omega_e L_s i_{s\alpha}}{\omega_e\, L_m}$$

`

$$i_{r\beta} = \frac{v_{s\alpha} - R_s\, i_{s\alpha} - \omega_e L_s i_{s\beta}}{\omega_e\, L_m}$$

The position of rotor current vector in the stationary reference frame can be computed as

$$\text{Sin } (\theta_1) = \frac{i_{r\alpha}}{\sqrt{(i_{r\alpha}^2 + i_{r\beta}^2)}}$$

$$\text{Cos } (\theta_1) = \frac{i_{r\beta}}{\sqrt{(i_{r\alpha}^2 + i_{r\beta}^2)}}$$

Step 3: From step1 and step2, the rotor position ($\varepsilon = \theta_1 - \theta_2$) can be obtained in terms of sin and cos. Knowing the unit vector sin (θ_1), cos (θ_1), sin (θ_2) and cos (θ_2), the rotor position unit vectors sin (ε) and Cos (ε) can be expressed

$$\text{Sin } (\varepsilon) = \sin (\theta_1) \cos (\theta_2) - \cos (\theta_1) \sin (\theta_2)$$

$$\text{Cos } (\varepsilon) = \cos (\theta_1) \cos (\theta_2) + \sin (\theta_1) \sin (\theta_2)$$

Rotor speed can be estimated by:

$$\omega_{r(est)} = \text{Cos } (\varepsilon) \frac{d}{dt} \text{Sin } (\varepsilon) - \text{Sin } (\varepsilon) \frac{d}{dt} \text{Cos } (\varepsilon)$$

Chapter 6

Simulation Results

6.1 Introduction

In this chapter the simulation results for the power control of DFIG using PI & FBLC are presented. Here we used wound rotor induction machine along with the rotor side and front end converter model using PI & FBLC is simulated using the MATLAB Simulink and the results are observed

6.2 Simulation results for the power control of DFIG using PI Control

The simulation results for the power control of DFIG using PI are presented in this section.

6.2.1 Simulation results for Sub-synchronous mode

In sub-synchronous mode the reference and actual stator active and reactive powers. At t = 2s the rotor side controller is switched ON, with the rotor speed constant at 1430 rpm. After switching on the controller following events occurs
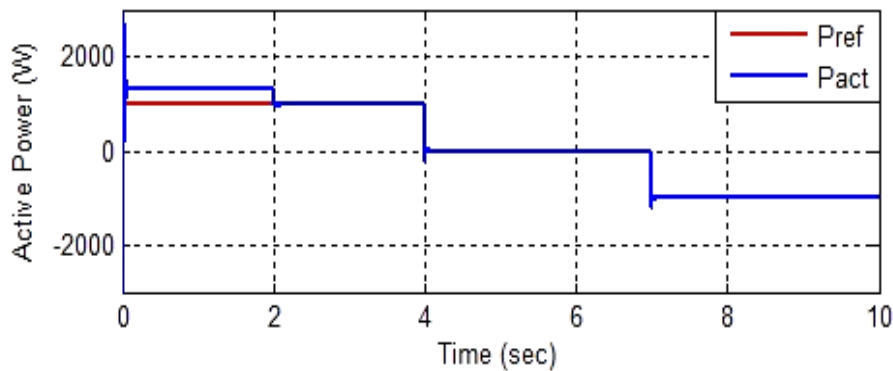
Fig 6.2.1 Reference and Actual active power
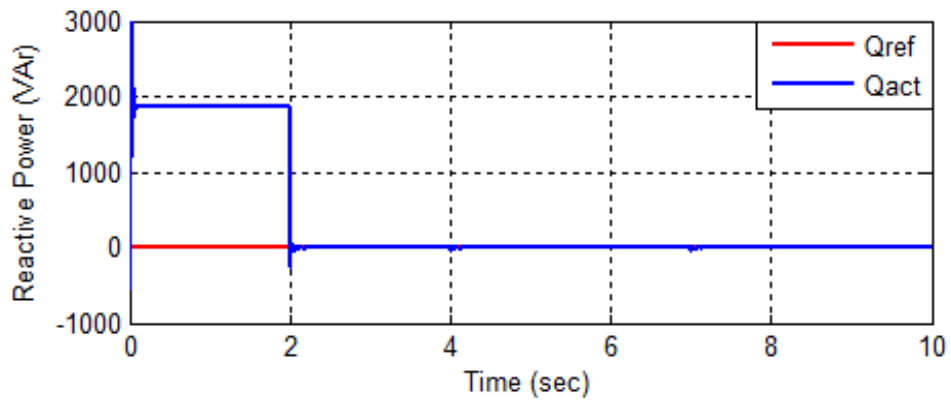
Fig 6.2.2 Reference and Actual Reactive power

The reference current of *d*-axis component is determined from the reactive power reference. After switching on the controller (at t = 2s), the variation of stator current *d*-axis component according to the variation in rotor current *d*-axis component shown below
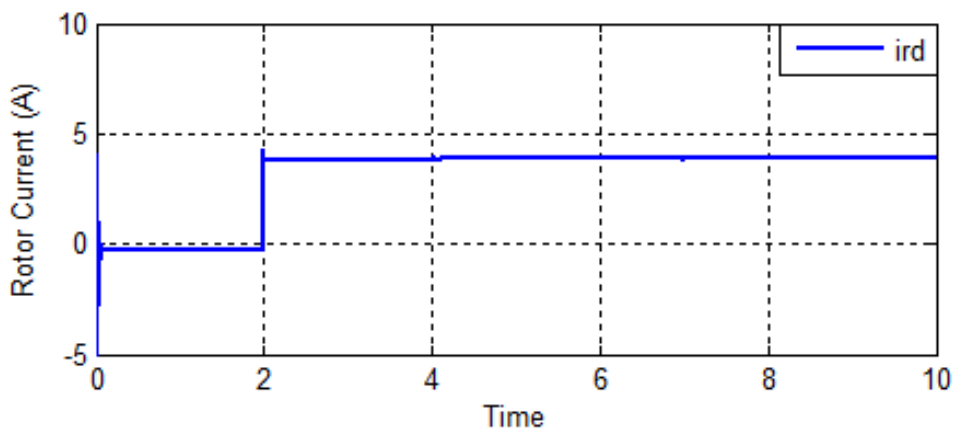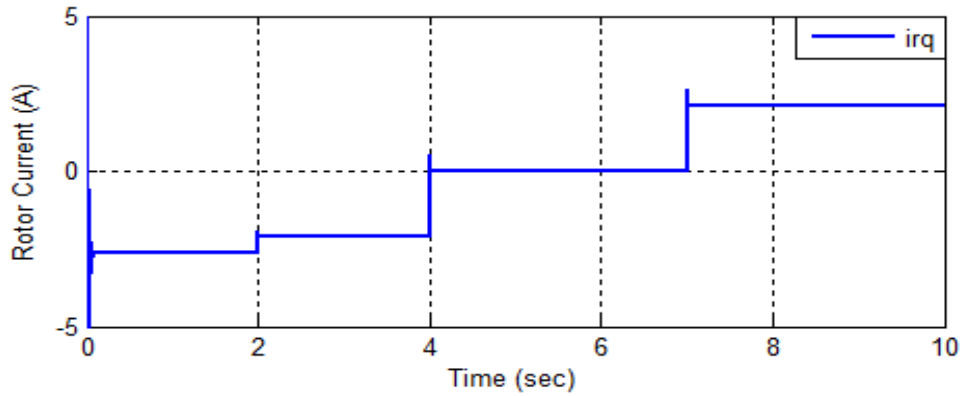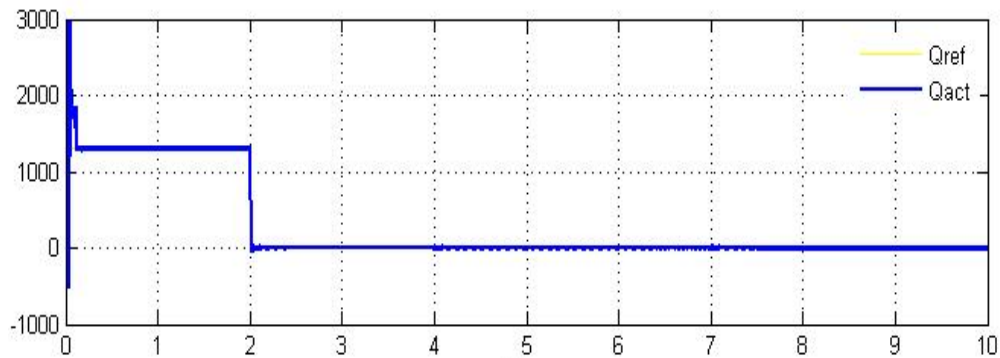

Fig 6.2.3 d-axis and Actual rotor current
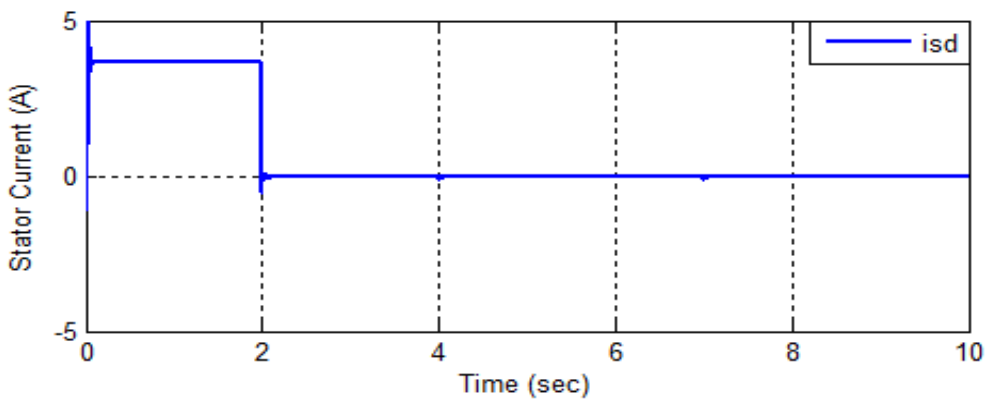
Fig 6.2.4 d-axis Actual stator current

The reference current of *q*-axis component is determined from the reactive power reference. After switching on the controller (at t = 2s), the variation of stator current *q*-axis component according to the variation in rotor current *q*-axis component shown below

Fig 6.2.5 q-axis Actual Rotor current
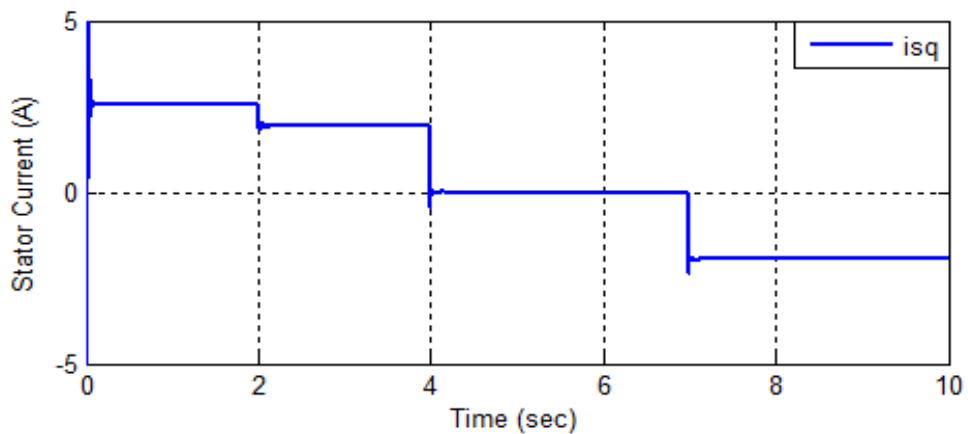
Fig 6.2.6 q-axis Actual Stator current

The *d*-axis component of voltage magnitude is determined from the *d*-axis component of rotor current according to reference reactive power. The *q*-axis component of voltage magnitude is determined from the *q*-axis component of rotor current according to reference active power Shown below
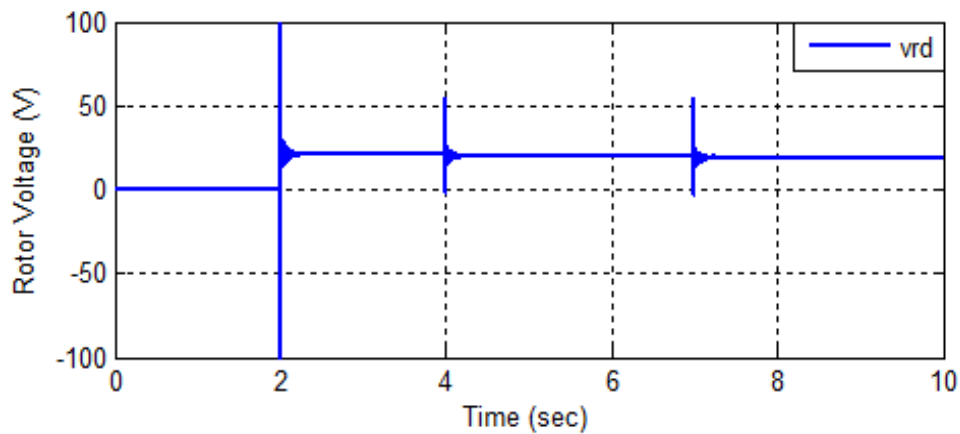
Fig 6.2.7 d-axis injection voltage
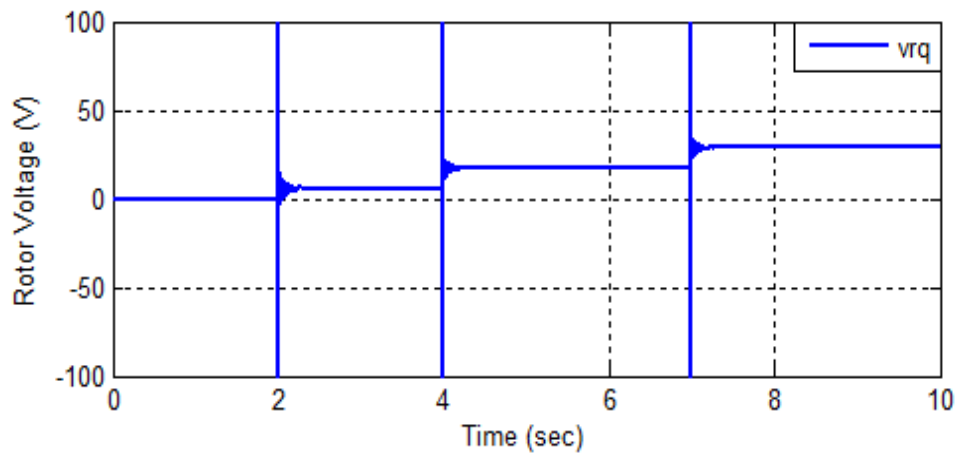
Fig 6.2.8 q-axis Injecting Voltage

6.3 Simulation results for the power control of DFIG using FBLC

The simulation results for the power control of DFIG using FBLC are presented in this section.

6.3.1 Simulation results for Sub-synchronous mode

In sub-synchronous mode the reference and actual stator active and reactive powers. At t = 2s the rotor side controller is switched ON, with the rotor speed constant at 1430 rpm. After switching on the controller following events occurs
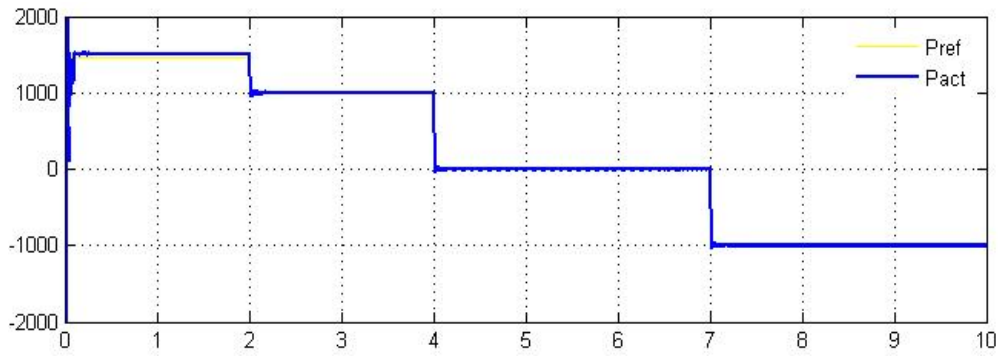
Fig 6.3.1 Reference and Actual active power

Fig 6.3.2 Reference and Actual Reactive power

The reference current of *d*-axis component is determined from the reactive power reference. After switching on the controller (at t = 2s), the variation of stator current *d*-axis component according to the variation in rotor current *d*-axis component shown below
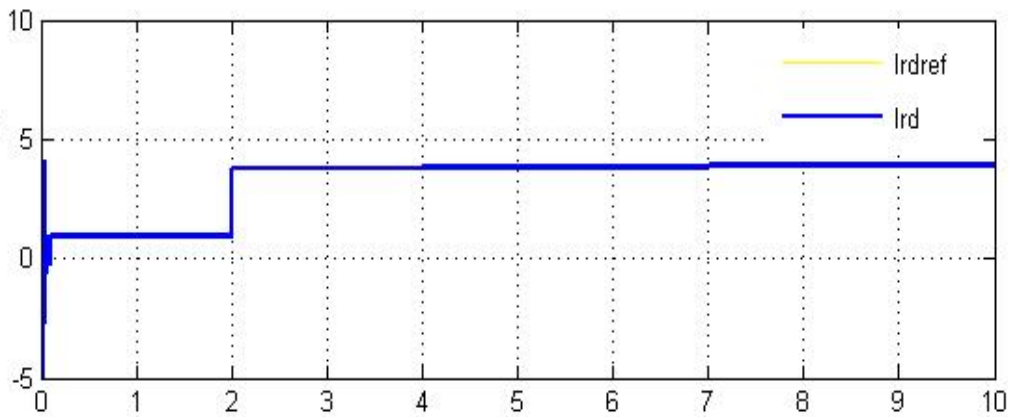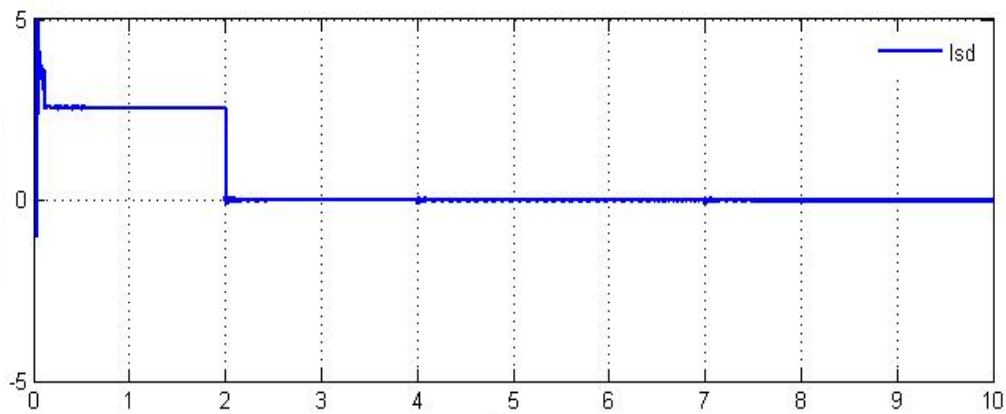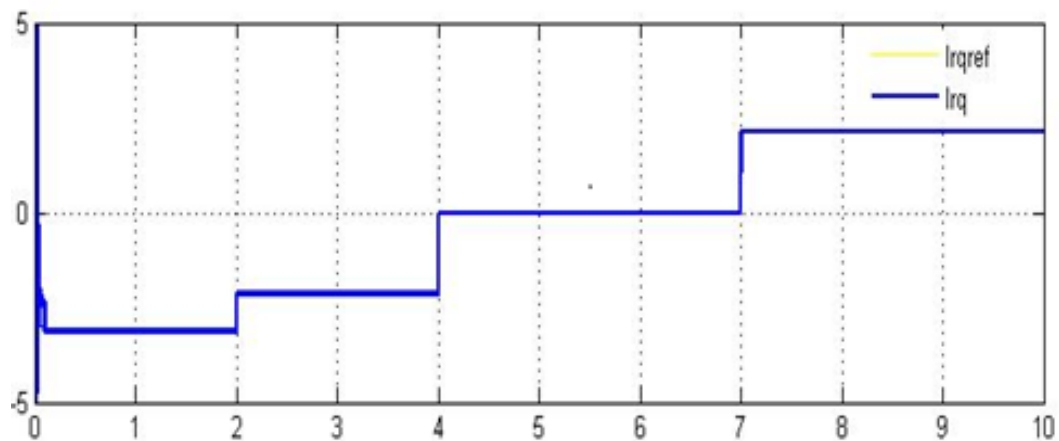

Fig 6.3.3 d-axis and Actual rotor current

Fig 6.3.4 d-axis Actual stator current

The reference current of q-axis component is determined from the reactive power reference. After switching on the controller (at t = 2s), the variation of stator current q-axis component according to the variation in rotor current q-axis component shown below
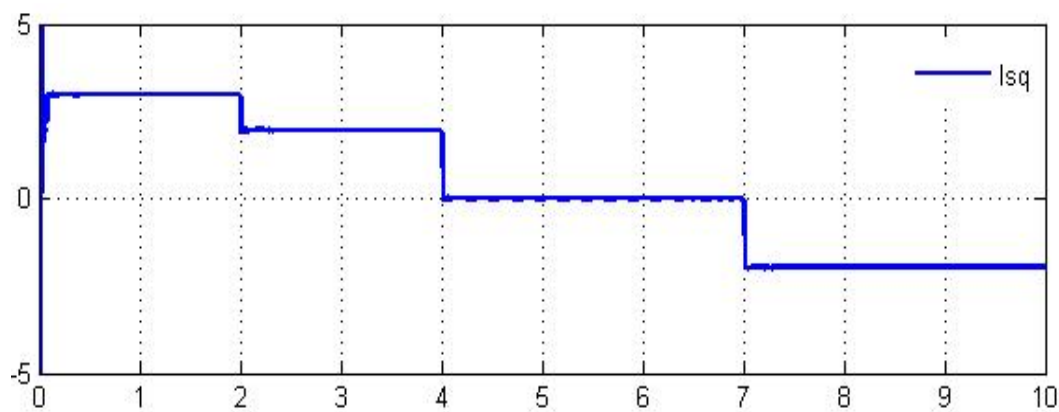

Fig 6.3.5 q-axis Actual Rotor current

Fig 6.3.6 q-axis Actual Stator current

The *d*-axis component of voltage magnitude is determined from the *d*-axis component of rotor current according to reference reactive power. The *q*-axis component of voltage magnitude is determined from the *q*-axis component of rotor current according to reference active power Shown below
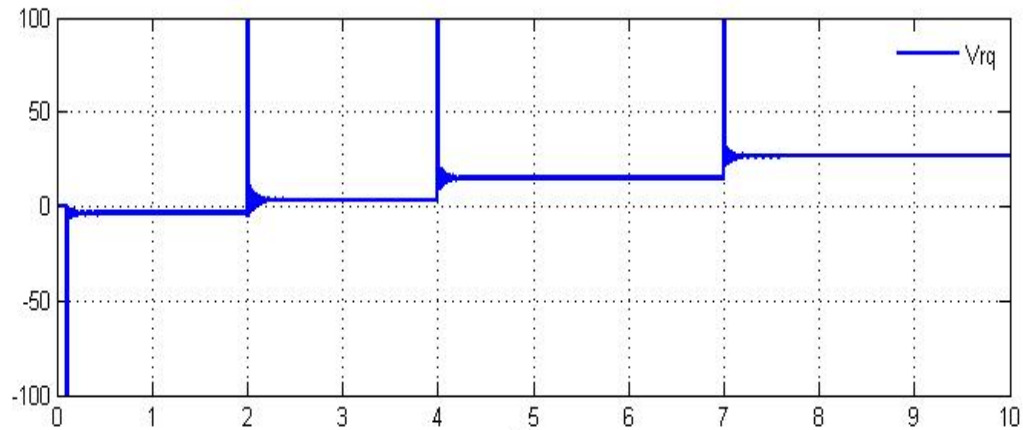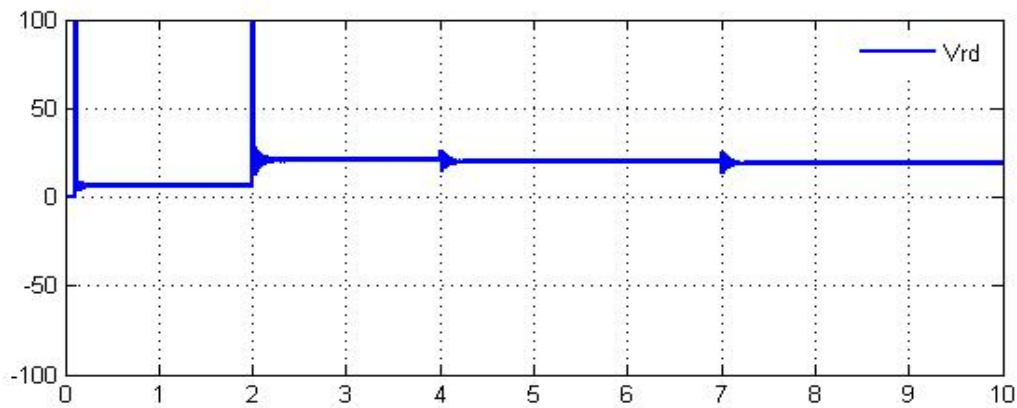

Fig 6.3.7 q-axis Injecting Voltage

Fig 6.3.8 d-axis Injection Voltage

6.4 Speed estimation and Position estimation

The stator current i_s, the rotor current i_r and the stator voltage v_s, are used for the estimation of rotor position and speed

6.4.1 Position estimation

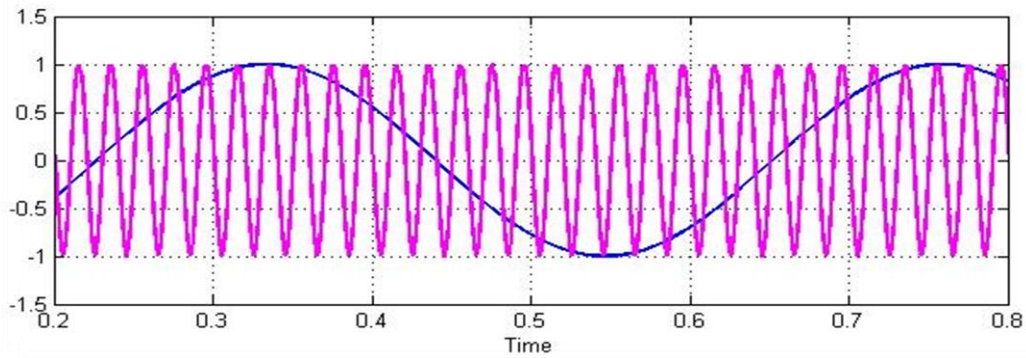The difference of θ_1-θ_2 is the Position of rotor (ε).

Fig 6.4.1 sin (θ₁) & sin (θ₂)   ----- Sin (θ₁)
                                                  ----- Sin (θ₂)

Fig 6.4.2 sin (ε)
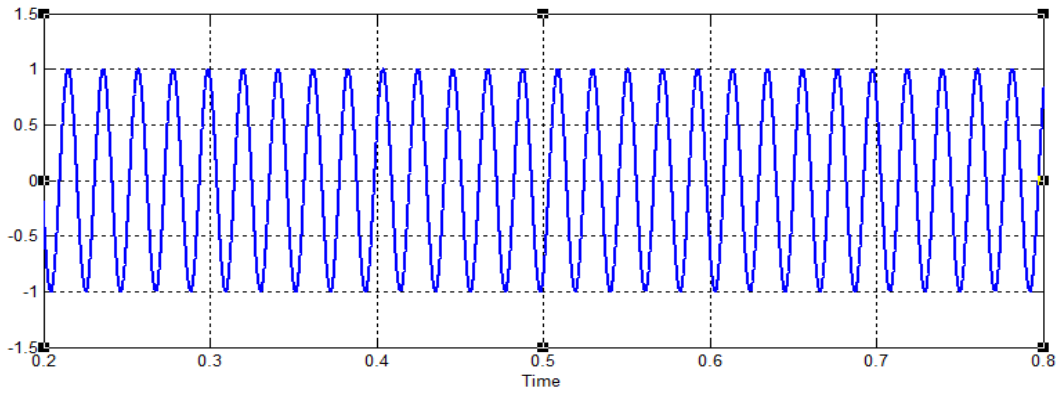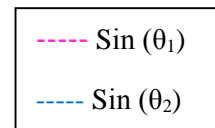
6.4.2 Speed estimation

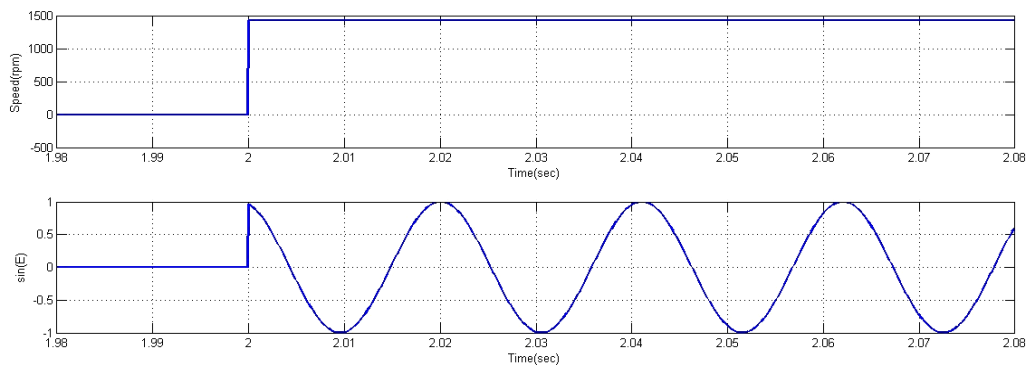The plot between sin (ε) and ω_{est}

Fig 6.4.3 sin (ε) and ω_{est}

Chapter 7

Conclusions

Power control of a doubly-fed induction generator using PI control is studied where mathematical model of DFIG is developed by extending the modelling of normal induction machine. The disadvantage of the PI control based control scheme such as relatively high oscillations in the rotor injected voltages are addressed using Feedback Linearization Control (FBLC) scheme. Reduction in the oscillations in rotor injected voltages is observed in case of FBLC thus achieving a better control.

A sensor less algorithm for rotor position and speed estimation is developed based on the reference produced from PI and FBLC is presented. The algorithm along with d-q model DFIG mathematical model are simulated in MATLAB/Simulink environment for both PI and FBLC control schemes.

.

Appendix

Induction Machine Parameters

Machine Specifications:

3 Hp, 414V, 50Hz, 3 Phase

Stator: 415V, Y connected, 4.7A

Rotor: 185V, Y connected, 7.5A

Machine Parameters

Parameter	Values
Stator resistance(R_s)	3.678Ω
Rotor Resistance(R_r)	5.26Ω
Stator Inductance(L_s)	306.82mH
Rotor Inductance(L_r)	306.82mH
Stator Leakage Inductance(L_{ls})	24.87mH
Rotor Leakage Inductance(L_{lr})	24.87mH
Magnetizing Inductance(L_0)	281.95mH

References

[1]. **R.Datta and V.T.Ranganathan**, "Direct power control of grid connected wound rotor induction machine without rotor position sensors," IEEE Trans. Power Electron., vol. 16, no. 3, pp. 390–399, May 2001

[2]. **John Fletcher** et al., "Introduction to Doubly-Fed Induction Generator for Wind Power Applications", University of Strathclyde, Glasgow, United Kingdom

[3]. **Muller, S., Deicke, M. & De Doncker, R.W.** (2002). Doubly fed induction generator systems for wind turbines, IEEE Ind. Appl. Magazine, Vol., No., May/June 2002, 26-33, ISSN 1077- 618/02

[4]. **R. Pena, J. C. Clare and G. M. Asher**, "Doubly fed induction generator using back-to-back PWM converts and its application to variable speed wind-energy generation," IEE Proceedings Electrical Power Application,Vol.143, pp. 231-241.1996

[5]. **Dong-Choon Lee, G-Myoung Lee, and Ki-Do Lee**, "DC-Bus Voltage Control of Three-Phase AC/DC PWM Converters Using Feedback Linearization", IEEE Transactions on Industry Applications, Vol. 36, No. 3, May/June 2000.

[6]. **B.Chitti Babu and K.B.Mohanty**, "Double-Fed Induction Generator for variable Speed Wind Energy Conversion Systems-Modeling & Simuation"International Journal of computer and Electrical Engineering", Vol. 2, No. 1, February, 2010 1793-8163

[7]. **Sheng Hu, DiHua Li, Yong Kang and XinChun Lin**,"Non-linear control strategy for double-fed induction generator(DFIG) in wind power control" IEEE 978-1-4244-4813-5/10, 2010

[8]. **C.Nagamani A.B Ray Chaudhary G.S. IIango**"Implicit position and speed estimation algorithm without the flux computation for the rotor side control of doubly fed induction motor drive"IET Electr. Power Appl.,2012, Vol.6, Iss.4, pp.243-252